

Free-breathing MRI of the upper abdomen assisted by motion modelling

Robert I Johnstone^{1,2}, David Atkinson³, Manil Chouhan³, Ricky A Sharma⁴, and Jamie R McClelland¹

¹Centre for Medical Image Computing, University College London, London, United Kingdom, ²Medical Physics, Guy's and St. Thomas' NHS Foundation Trust, London, United Kingdom, ³Centre for Medical Imaging, University College London, London, United Kingdom, ⁴NIHR University College London Hospitals Biomedical Research Centre, University College London, London, United Kingdom

Synopsis

This study demonstrates the use of motion modelling and super resolution reconstruction (SRR) to produce an isotropic 3D image of the upper abdomen during free breathing.

Sagittal and coronal 6 mm 2D slices are acquired throughout the volume of interest. The slices are repeated with sub-voxel offsets to facilitate SRR. An interleaved navigator slice is also acquired.

The navigator slice is processed with non-rigid registration and principal component analysis, to give two motion surrogate signals. These signals are used to control the motion model. The motion model and the SRR are jointly optimised using an iterative scheme.

Introduction

Clinical MRI of the upper abdomen usually involves multiple breathholds in order to obtain T2-weighted 2D images that are aligned to one another. When breath-holds are imperfect or inconsistent, there are stacking artefacts between the image slices. Figure 1 shows an example where two breath-holds were inconsistent. This study demonstrates the use of respiratory motion modelling and super-resolution reconstruction (SRR) to remove stacking artefacts and produce a 3D volume image with isotropic spatial resolution.

Methods

A volunteer was scanned, breathing freely, on a Philips Ingenia 3T system with dStream torso coil. A 2D single-shot half-Fourier turbo spin-echo (TSE) sequence was used with TE = 90 ms. Signal from fat was suppressed with spatial pre-saturation with inversion recovery (SPIR).

Contiguous stacks of sagittal and coronal 6 mm image slices were acquired through the abdomen and thorax. The stacks were repeated with a 2 mm and a 4 mm offset in the through-slice direction, to allow SRR. The in-plane acquired voxel sizes were 2.0 × 2.0 mm. Interleaved with every image slice was a sagittal navigator slice, positioned through the right hemi-diaphragm. The complete sagittal and coronal stacks were acquired five and four times, respectively, and the total acquisition time was 25 minutes.

The navigator slices were registered to a group average image using non-rigid registration¹. Principal component analysis (PCA) was applied to a matrix of the deformation fields over time. The weights of the first two principal components were converted to standard scores and then interpolated with a cubic spline to the acquisition time of the image slices. The interpolated values were used as motion surrogate signals.

A method which combines respiratory motion modelling and image registration was used to fit a 3D motion model directly to the 2D image slices². The motion model was used to perform a motion compensated SRR using the iterative back projection method³. The motion model and SRR were jointly optimised using an iterative scheme². The voxel spacing in the motion-compensated image was an isotropic 1.875 mm.

Results

Slices through the motion-corrected reconstructed 3D image are shown in Figure 2 and a non-motion compensated reconstruction is shown in Figure 3, for comparison. Figure 4 shows slices displayed at a higher magnification through the gall bladder and the biliary tree, with non-motion compensated images in Figure 5.

The reconstruction has effectively removed the slice stacking artefacts that would normally be seen when reconstructing a 3D volume from 2D images acquired during free breathing. The liver, gall bladder and bile ducts are displayed clearly in Figures 2 and 4, but blurred in Figure 3 and 5, indicating that the motion model has successfully compensated for the respiratory motion.

Discussion

The results show that a clinically useful improvement in image quality and resolution can be obtained using the proposed method. However, further improvements are required before the method is suitable for routine clinical use.

In 2D TSE imaging, the signal from flowing blood varies, depending on the flow velocity and the direction of flow compared to the slice plane. This means that the signal from the blood is different for the sagittal and coronal images that are used for the reconstruction. This is likely to cause errors in the motion model. The inconsistent blood signal was confirmed by the radiologist in the team.

A high specific absorption rate (SAR) was experienced by the volunteer, due to the use of a TSE sequence. This was a significant limitation to the speed of the acquisition, adding 89% to the scan time. The 2D imaging sequence used was a T2-weighted half-Fourier turbo spin echo sequence, but any single-shot 2D sequence could have been used to achieve different image contrasts and, potentially, a lower SAR.

The use of an interleaved navigator slice with the same image quality as the image slices means that only half of the acquired data is used to generate the final image. The acquisition time could therefore be halved by obtaining motion surrogate signals that are independent of the imaging process or are derived from thermal noise in the receive coils⁴.

Conclusion

We have demonstrated that respiratory motion models can effectively remove stacking artefacts from 2D MRI of the upper abdomen. SRR allowed recovery of high spatial frequencies in the through-slice direction.

Acknowledgements

This work is supported by the EPSRC-funded UCL Centre for Doctoral Training in Medical Imaging (EP/L016478/1).

References

1. Modat M, Ridgway GR, Taylor ZA, Lehmann M, Barnes J, Hawkes DJ, Fox NC, and Ourselin S. Fast freeform deformation using graphics processing units. *Comput Meth Prog Bio.* 2010;98(3):278–284,.
2. McClelland JR, Modat M, Arridge S, Grimes H, D’Souza D, Thomas D, O’Connell D, Low DA, Kaza E, Collins DJ, Leach MO, and Hawkes DJ. A generalized framework unifying image registration and respiratory motion models and incorporating image reconstruction, for partial image data or full images. *Phys Med Biol.* 2017;62:4273–4292.
3. Irani M and Peleg S. Motion analysis for image enhancement: Resolution, occlusion, and transparency. *J Vis Commun Image R.* 1993;4(4):324–335
4. Andreychenko A, Raaijmakers AJE, Sbrizzi A, Crijns SPM, Lagendijk JJW, Luijten PR, and van den Berg CAT. Thermal noise variance of a receive radiofrequency coil as a respiratory motion sensor. *Magn Reson Med.* 2017;77(1):221–228.

Figures

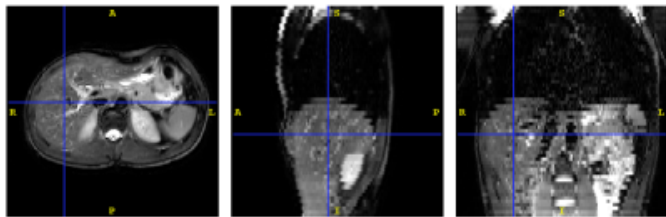


Figure 1: Slices taken through a naïve 3D reconstruction of a stack of transverse 2D slices through the torso and abdomen. Left to right: transverse, sagittal and coronal slices. The blue lines indicate the intersection of the three planes. The acquisition is a 2D single-shot half-Fourier turbo spin-echo (TSE) sequence, with TE = 90 ms, 6 mm slice thickness and no slice gap. The slices were acquired in an interleaved order, with two breath holds. Nearest neighbour interpolation is used between pixels.

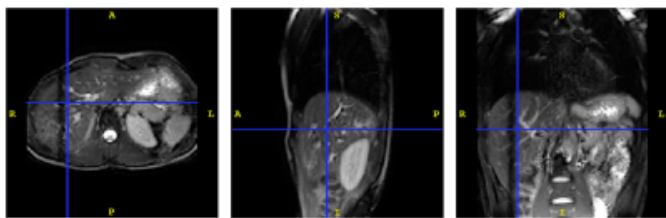


Figure 2: Slices through the motion compensated reconstruction. Left to right: transverse, sagittal and coronal slices. The blue lines indicate the intersection of the three planes. The sharp boundary at the interface between the lungs and the liver demonstrates the effectiveness of the motion model at removing breathing motion. The dark band seen in the transverse and coronal images shows the magnetic saturation effect of the interleaved navigator slice. Nearest neighbour interpolation is used between pixels.

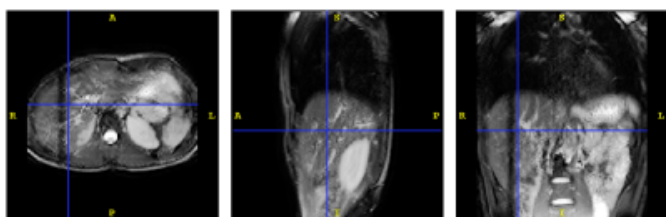


Figure 3: Slices through a reconstruction without motion compensation. Left to right: transverse, sagittal and coronal slices. The blue lines indicate the intersection of the three planes.

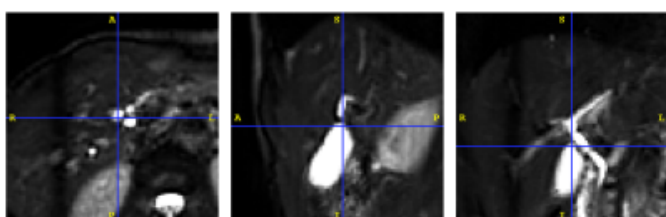


Figure 4: Enlarged view of the motion compensated reconstruction, to show the gall bladder and adjacent ducts. Left to right: transverse, sagittal and coronal slices. The blue lines indicate the intersection of the three planes. The transverse view shows three closely-spaced hyperintense areas, with the left-most being the superior extremity of the gall bladder, the inferior being the cystic duct and the superior being the common hepatic duct. Windowing was chosen for good visualisation of the ducts and gall bladder. Nearest neighbour interpolation is used between pixels.

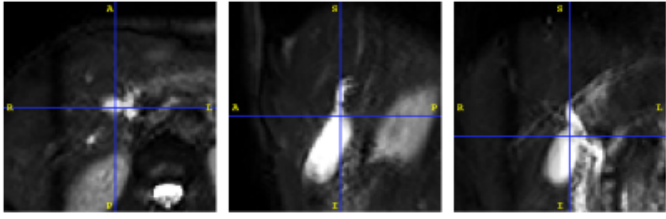


Figure 5: Enlarged view of the non-motion compensated reconstruction, to show the gall bladder and adjacent ducts. Left to right: transverse, sagittal and coronal slices. The blue lines indicate the intersection of the three planes.